

**NGU REPORT
2015.040**

Helicopter-borne magnetic and
radiometric geophysical survey at Kviteseid,
Nissedal, Fyresdal and Dalen,
Telemark County

Report no.: 2015.040		ISSN: 0800-3416 (print) ISSN: 2387-3515 (online)		Grading: Open	
Title: Helicopter-borne magnetic and radiometric geophysical survey at Kviteseid, Nissedal, Fyresdal and Dalen, Telemark county					
Authors: Alexandros Stampolidis and Frode Ofstad			Client: NGU / Regionaleologen for BTV		
County: Telemark			Commune: Kviteseid, Nissedal, Fyresdal og Tokke		
Map-sheet name (M=1:250.000) SAUDA and SKIEN			Map-sheet no. and -name (M=1:50.000) 1513 I Bandak, 1513 II Fyresvatnet 1513 III Grøssæ, 1513 IV Dalaen		
Deposit name and grid-reference: Fyresdal WGS 84, UTM zone 32V, 450000 E, 6560000 N			Number of pages: 30 Price (NOK): 120,- Map enclosures:		
Fieldwork carried out: June 2015		Date of report: August 13 th 2015		Project no.: 353200	
				Person responsible: <i>Jan S. Rønning</i>	
Summary: <p>NGU conducted an airborne magnetic and radiometric survey at Kviteseid, Nissedal, Fyresdal and Dalen, Telemark county in June 2015 as a part of the MINS project (Mineral resources in Southern Norway). This report describes and documents the acquisition, processing and visualization of recorded datasets. The geophysical survey results reported herein are approximately 7340 line km, covering an area of approximately 1468 km².</p> <p>A helicopter-borne system (AS350 B2) designed to obtain detailed airborne magnetic and radiometric data was used in this survey. It had a Scintrex Cs-3 magnetometer in a towed bird and a 1024 channels RSX-5 spectrometer installed under the helicopter belly.</p> <p>The survey was flown with 200 m line spacing. The flight line direction was east-west (EW). The average speed for the survey was about 82 km/h and was ranged between 40 and 140 km/h depending, mainly, on the local topography. The average terrain clearance of the bird was about 55 m and about 80m for the spectrometer.</p> <p>Collected data were processed at NGU using Geosoft Oasis Montaj software. Raw total magnetic field data were corrected for diurnal variations, the IGRF was calculated and subtracted and then the total field anomaly data were levelled using standard micro-levelling algorithm. Radiometric data were processed using standard procedures recommended by International Atomic Energy Association (IAEA).</p> <p>Data were gridded with a cell size of 50 x 50 m and presented as shaded relief maps at scale of 1:100.000.</p>					
Keywords: Geophysics		Airborne		Magnetic	
		Gamma spectrometry		Radiometric	
				Technical report	

CONTENTS

- 1. INTRODUCTION 7**
- 2. SURVEY SPECIFICATIONS 8**
 - 2.1 Airborne Survey Parameters 8**
 - 2.2 Airborne Survey Instrumentation 9**
 - 2.3 Airborne Survey Logistics Summary 10**
- 3. DATA PROCESSING AND PRESENTATION 11**
 - 3.1 Total Field Magnetic Data 11**
 - 3.2 Radiometric data 13**
- 4. PRODUCTS 17**
- 5. REFERENCES 18**

- 6. APPENDIX..... 19**
 - A1 Flow chart of magnetic processing..... 19**
 - A2 Flow chart of radiometry processing 19**

FIGURES

- Figure 1: Surveyed areas..... 7**
- Figure 2: Photo of Heliscan’s Eurocopter AS350-B2 (P1)..... 10**
- Figure 3: An example of Gamma-ray spectrum..... 13**
- Figure 4: Flight path map 21**
- Figure 5: Total Magnetic Field anomaly map..... 22**
- Figure 6: Magnetic Horizontal Gradient map 23**
- Figure 7: Magnetic Vertical Gradient map..... 24**
- Figure 8: Magnetic Tilt Derivative map 25**
- Figure 9: Radiometry: Total Counts map..... 26**
- Figure 10: Potassium Ground Concentration map..... 27**
- Figure 11: Uranium Ground Concentration map 28**
- Figure 12: Thorium Ground Concentration map..... 29**
- Figure 13: Ternary Image of Radiation Concentration 30**

TABLES

- Table 1. Flight specifications of the surveyed areas 7**
- Table 2. Instrument Specifications 9**
- Table 3. Survey Specifications Summary 10**
- Table 4. Specified channel windows for the 1024 RSX-5 systems..... 13**
- Table 5. Maps available from NGU on request. 17**

1. INTRODUCTION

In 2013 the Norwegian government initiated a new program for mapping of mineral resources in Southern Norway (MINS). The goal of this program is to enhance the geological information that is relevant to an assessment of the mineral potential. The airborne geophysical surveys - helicopter borne and fixed wing- are important integral parts of MINS program. The airborne survey results reported herein amount about 7340 line km (1500 km²) over the surveyed areas, as shown in Figure 1.

The surveyed area was flown at a E-W direction (90°).



Figure 1: Map of southern Norway. The black polygon marks the borders of the surveyed area.

Table 1. Flight specifications

Name	Surveyed lines (km)	Surveyed area (Km ²)	Flight direction	Average flight speed (km/h)
Kviteseid, Nissedal, Fyresdal and Dalen	7340	1500	E-W	82

The objective of the airborne geophysical survey was to obtain a dense high-resolution aero-magnetic and radiometric data set over the survey area. These data sets are required for the enhancement of a general understanding of the regional geology. In this regard, the data can also be used to map contacts and structural features within the area. It also improves defining the potential of known zones of mineralization, their geological settings, and identifying new areas of interest.

The survey incorporated the use of a high-sensitivity Cesium magnetometer, gamma-ray spectrometer and radar altimeter. GPS navigation computer systems with flight path indicators ensured accurate positioning of the geophysical data with respect to the World Geodetic System 1984 geodetic datum (WGS-84).

2. SURVEY SPECIFICATIONS

2.1 Airborne Survey Parameters

A helicopter-borne system designed to obtain detailed airborne magnetic and radiometric data used in the 2015 year survey. The system uses a Scintrex Cs-3 magnetic sensor housed in a 2m long bird towed 30 meters below the helicopter to record the total magnetic field and a 1024 channel gamma-ray spectrometer installed under the helicopter belly to map ground concentrations of Uranium, Thorium and Potassium.

The airborne survey began on June 5th and ended on June 26th 2015. A Eurocopter AS350-B2 from helicopter company HeliScan AS was employed. The survey lines were spaced 200 m apart throughout the survey while their flight direction was E-W. Instrument operation was performed by Heliscan AS employees.

Large water bodies, rugged terrain and abrupt changes in topography affected the pilot's ability to 'drape' the terrain; therefore there are positive and negative variations in sensor height with respect to the standard helicopter height, which is defined as 60 m plus a height of obstacles (trees, power lines). The average survey height for the magnetic sensor was about 55 m, while for the spectrometer it was about 80m. Due to flight safety rules parts on some profiles were flown at altitudes higher than 150m. Those data were discarded during the radiometric processing.

The ground speed of the helicopter varied from 40–140 km/h depending on topography, wind direction and its magnitude. On average the ground speed during the whole survey was about 82 km/h.

Magnetic data were recorded at 0.2 second intervals resulting in average point spacing of 4.5 m. Spectrometry data were recorded every 1 second giving a point spacing of approximately 22.5 meters.

The above parameters were designed to allow for sufficient details in the data to detect subtle anomalies that may represent mineralization and/or rocks of different lithological and petro-physical composition.

A base magnetometer to monitor diurnal variations in the magnetic field was installed close to the helicopter base at Eidstod, during the survey period. A GEM GSM-19 magnetometer that recorded data every 3 seconds was employed. The CPU clock of the magnetometers was synchronized through the built-in GPS receiver to permit synchronization with the recorded airborne magnetic data and subsequent removal of diurnal drift from them.

Navigation system uses GPS/GLONASS satellite tracking systems to provide real-time WGS-84 coordinate locations for every second. The accuracy achieved with no differential corrections is reported to be less than ± 5 m in the horizontal directions. The GPS receiver antenna was mounted externally to the tail tip of the helicopter.

For quality control, the magnetic, radiometric, altitude and navigation data were monitored on two separate windows in the operator's display during flight while they were recorded in ASCII data streams to the acquisition's PC hard disk drive.

2.2 Airborne Survey Instrumentation

Instrument specifications are given in table 2.

Table 2. *Instrument Specifications*

Instrument	Producer/Model	Accuracy / Sensitivity	Sampling frequency / interval
Magnetometer	Scintrex Cs-3	<2.5nT throughout range / 0.002nT	5 Hz
Base magnetometer	GEM GSM-19	0.1 nT	3 s
Gamma spectrometer	Radiation Solutions RSX-5	1024 ch's, 16 liters down, 4 liters up	1 Hz
Radar altimeter	Bendix/King KRA 405B	$\pm 3\%$ 0 – 500 feet $\pm 5\%$ 500 – 2500 feet	1 Hz
Pressure/temperature	Honeywell PPT	$\pm 0.03\%$ FS	1 Hz
Navigation	Topcon GPS-receiver	± 5 meter	1 Hz
Acquisition system	NGU custom software		

The magnetic, radiometric, altitude and navigation data were monitored on the operator's displays during flight while they were recorded to the PC's hard disk drive. Spectrometry data were also recorded to internal hard drive of the spectrometer. The data files were transferred to the field workstation via USB flash drive. The raw data files were backed up onto USB flash drive in the field.

2.3 Airborne Survey Logistics Summary

A summary of the survey specifications is shown in Table 3.

Table 3. Survey Specifications Summary

Parameter	Specifications
Traverse (survey) line spacing	200 metres
Traverse line direction	E-W (90°)
Nominal aircraft ground speed	40 - 140 km/h
Average aircraft ground speed	82 km/h
Average sensor terrain clearance Mag	55m
Average sensor terrain clearance Rad	80m
Sampling rates:	
Magnetometer	0.2 seconds
Spectrometer, GPS, altimeter	1.0 second



Figure 2: Photo of Heliscan's Eurocopter AS350-B2 (P1). The Mag bird in front of the helicopter and the spectrometer under its belly are also depicted.

3. DATA PROCESSING AND PRESENTATION

All data were processed by Alexandros Stampolidis at NGU. The ASCII data files were loaded into separate Oasis Montaj databases. The datasets were processed consequently according to processing flow charts shown in Appendix A1 and A2.

3.1 Total Field Magnetic Data

At the first stage the raw magnetic data were checked for spikes, using the 4th difference calculation as a flag. Obvious spikes were checked and then manually removed. The data from base stations were also inspected for spikes and spikes were removed manually if necessary. Typically, several corrections have to be applied to magnetic data before gridding – i.e. heading, lag and diurnal correction.

Diurnal Corrections

The temporal fluctuations in the magnetic field of the earth affect the total magnetic field readings during the airborne survey. This is commonly referred to as the magnetic diurnal variation. These fluctuations can be effectively removed from the airborne magnetic dataset by using a stationary reference magnetometer that records the magnetic field of the earth at a given short time interval. Magnetic diurnals that were recorded on the base station magnetometer, were within the standard NGU specifications during the entire survey (Rønning 2013).

Diurnal variations were measured with a GEM GSM-19 base station magnetometer. The base station computer clock was continuously synchronized with GPS clock. The recorded data are merged with the airborne data and the diurnal correction is applied according to equation (1).

$$\mathbf{B}_{Tc} = \mathbf{B}_T + (\bar{\mathbf{B}}_B - \mathbf{B}_B), \quad (1)$$

Where:

\mathbf{B}_{Tc} = Corrected airborne total field readings

\mathbf{B}_T = Airborne total field readings

$\bar{\mathbf{B}}_B$ = Average datum base level

\mathbf{B}_B = Base station readings

The average datum base level ($\bar{\mathbf{B}}_B$) was set equal to 50713.45 nT.

Corrections for Lag and heading

Neither a lag nor cloverleaf tests were performed before the survey. According to previous reports the lag between logged magnetic data and the corresponding navigational data was 1-2 fids. Translated to a distance it would be no more than 10 m - the value comparable with the precision of GPS. A heading error for a towed system is usually either very small or non-existent. So no lag and heading corrections were applied.

Magnetic data processing, gridding and presentation

The total field magnetic anomaly data (\mathbf{B}_{TA}) were calculated from the diurnal corrected data (\mathbf{B}_{Tc}) after subtracting the IGRF for the surveyed area calculated for the data period (eq.2)

$$\mathbf{B}_{TA} = \mathbf{B}_{Tc} - IGRF \quad (2)$$

IGRF 2015 model was employed in these calculations.

The total field anomaly data were split into lines and then were gridded using a minimum curvature method with a grid cell size of 50 meters. This cell size is equal to one quarter of the 200m average line spacing. In order to remove small line-to-line levelling errors that were detected on the gridded magnetic anomaly data, the Geosoft Micro-levelling technique was applied on the flight line based magnetic database. Then, the micro-levelled channel was gridded using again a minimum curvature method with 50 m grid cell size.

The processing steps of magnetic data presented so far were performed on point basis. The following steps are performed on grid basis:

The Horizontal and Vertical Gradient along with the Tilt Derivative of the total magnetic anomaly were calculated from the stitched micro-levelled total magnetic anomaly grid. The magnitude of the horizontal gradient was calculated according to equation (3)

$$HG = \sqrt{\left(\frac{\partial(B_{TA})}{\partial x}\right)^2 + \left(\frac{\partial(B_{TA})}{\partial y}\right)^2} \quad (3)$$

where \mathbf{B}_{TA} is the micro-levelled total field anomaly field. The vertical gradient (VG) was calculated by applying a vertical derivative convolution filter to the micro-levelled \mathbf{B}_{TA} field. The Tilt derivative (TD) was calculated according to the equation (4)

$$TD = \tan^{-1}\left(\frac{VG}{HG}\right) \quad (4)$$

A 5x5 convolution filter was applied to smooth the resulted magnetic grids.

The results are presented in a series of colored shaded relief maps (1:100.000). The maps are:

- A. Total field magnetic anomaly
- B. Horizontal gradient of total magnetic anomaly
- C. Vertical gradient of total magnetic anomaly
- D. Tilt Derivative (or Tilt angle) of the total magnetic anomaly

They are representative of the distribution of magnetization over the surveyed area. A list of the produced maps is shown in Table 5.

3.2 Radiometric data

Airborne gamma-ray spectrometry measures the abundance of Potassium (K), Thorium (eTh), and Uranium (eU) in rocks and weathered materials by detecting gamma-rays emitted due to the natural radioelement decay of these elements. The data analysis method is based on the IAEA recommended method for U, Th and K processing (International Atomic Energy Agency, IAEA 1991; IAEA 2003). A short description of the individual processing steps of that methodology as adopted by NGU is given below.

Energy windows

The Gamma-ray spectra were initially reduced into standard energy windows corresponding to the individual radio-nuclides K, U and Th. Figure 3 shows an example of a Gamma-ray spectrum and the corresponding energy windows and radioisotopes (with peak energy in MeV) responsible for the radiation.

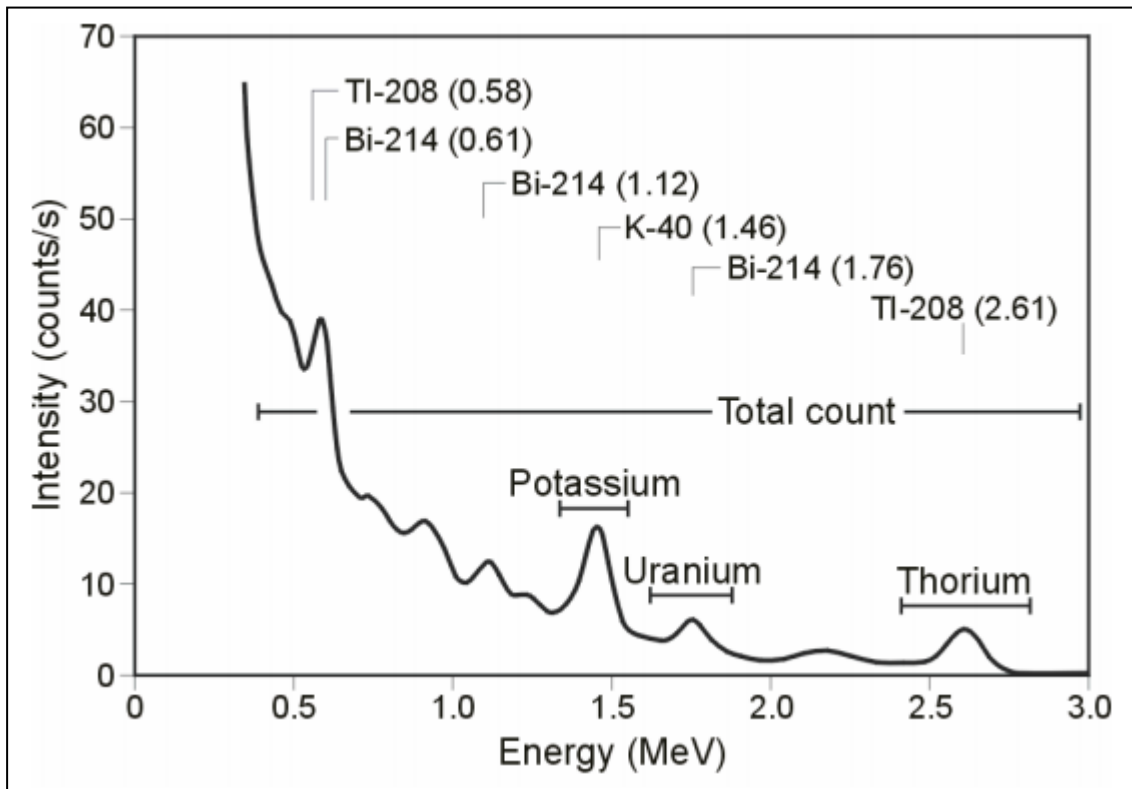


Figure 3: An example of Gamma-ray spectrum showing the position of the K, Th, U and Total count windows.

Table 4. Specified channel windows for the 1024 RSX-5 system used in this survey

Gamma-ray spectrum	Cosmic	Total count	K	U	Th
Down	1022	134-934	454-521	550-617	801-934
Up	1022			550-617	
Energy windows (MeV)	>3.07	0.41-2.81	1.37-1.57	1.66-1.86	2.41-2.81

The RSX-5 is a 1024 channel system with four downward and one upward looking detector, which means that the actual Gamma-ray spectrum is divided into 1024 channels. The first channel is reserved for the “Live Time” and the last for the Cosmic rays. Table 4 shows the channels that were used for the reduction of the spectrum.

Live Time correction

The data were corrected for live time. “Live time” is an expression of the relative period of time the instrument was able to register new pulses per sample interval. On the other hand “dead time” is an expression of the relative period of time the system was unable to register new pulses per sample interval. The relation between “dead” and “live time” is given by the equation (5)

$$\text{“Live time”} = \text{“Real time”} - \text{“Dead time”} \quad (5)$$

where the “real time” or “acquisition time” is the elapsed time over which the spectrum is accumulated (about 1 second).

The live time correction is applied to the total count, Potassium, Uranium, Thorium, upward Uranium and cosmic channels. The formula used to apply the correction is as follows:

$$C_{LT} = C_{RAW} \cdot \frac{\text{Acquisition Time}}{\text{Live Time}} \quad (6)$$

where C_{LT} is the live time corrected channel in counts per second, C_{RAW} is the raw channel data in counts per second, while Acquisition Time and Live Time are in microseconds.

Cosmic and aircraft correction

Background radiation resulting from cosmic rays and aircraft contamination was removed from the total count, Potassium, Uranium, Thorium, upward Uranium channels using the following formula:

$$C_{CA} = C_{LT} - (a_c + b_c \cdot C_{Cos}) \quad (7)$$

where C_{CA} is the cosmic and aircraft corrected channel, C_{LT} is the live time corrected channel a_c is the aircraft background for this channel, b_c is the cosmic stripping coefficient for this channel and C_{Cos} is the low pass filtered cosmic channel.

Radon correction

The upward detector method, as discussed in IAEA (1991), was applied to remove the effects of the atmospheric radon in the air below and around the helicopter. Using spectrometry data over-water, where there is no contribution from the ground sources, enables the calculation of the coefficients (a_c and b_c) for the linear equations that relate the cosmic corrected counts per second of Uranium channel with that of total count, Potassium, Thorium and Uranium upward channels over water. Data over-land was used in conjunction with data over-water to calculate the a_1 and a_2 coefficients used in equation (8) for the determination of the Radon component in the downward uranium window:

$$Radon_U = \frac{U_{up_{CA}} - a_1 \cdot U_{CA} - a_2 \cdot Th_{CA} + a_2 \cdot b_{Th} - b_U}{a_U - a_1 - a_2 \cdot a_{Th}} \quad (8)$$

where $Radon_U$ is the radon component in the downward Uranium window, $U_{up_{CA}}$ is the filtered upward uranium, U_{CA} is the filtered Uranium, Th_{CA} is the filtered Thorium, a_1 , a_2 , a_U and a_{Th} are proportional factors and b_U and b_{Th} are constants determined experimentally.

The effects of Radon in the downward Uranium are removed by simply subtracting $Radon_U$ from U_{CA} . The effects of radon in the other channels are removed using the following formula:

$$C_{RC} = C_{CA} - (a_C \cdot Radon_U + b_C) \quad (9)$$

where C_{RC} is the Radon corrected channel, C_{CA} is the cosmic and aircraft corrected channel, $Radon_U$ is the Radon component in the downward uranium window, a_C is the proportionality factor and b_C is the constant determined experimentally for this channel from over-water data.

Compton Stripping

Potassium, Uranium and Thorium Radon corrected channels, are subjected to spectral overlap correction. Compton scattered gamma rays in the radio-nuclides energy windows were corrected by window stripping using Compton stripping coefficients determined from measurements on calibrations pads (Grasty et al. 1991) at the Geological Survey of Norway in Trondheim (see values in Appendix A2).

The stripping corrections are given by the following formulas:

$$A_1 = 1 - (g \cdot \gamma) - (a \cdot \alpha) + (a \cdot g \cdot \beta) - (b \cdot \beta) + (b \cdot \alpha \cdot \gamma) \quad (10)$$

$$U_{ST} = \frac{Th_{RC} \cdot ((g \cdot \beta) - \alpha) + U_{RC} \cdot (1 - b \cdot \beta) + K_{RC} \cdot ((b \cdot \alpha) - g)}{A_1} \quad (11)$$

$$Th_{ST} = \frac{Th_{RC} \cdot (1 - (g \cdot \gamma)) + U_{RC} \cdot (b \cdot \gamma - a) + K_{RC} \cdot ((a \cdot g) - b)}{A_1} \quad (12)$$

$$K_{ST} = \frac{Th_{RC} \cdot ((\alpha \cdot \gamma) - \beta) + U_{RC} \cdot ((a \cdot \beta) - \gamma) + K_{RC} \cdot (1 - (a \cdot \alpha))}{A_1} \quad (13)$$

where U_{RC} , Th_{RC} , K_{RC} are the radon corrected Uranium, Thorium and Potassium and a , b , g , α , β , γ are Compton stripping coefficients. U_{ST} , Th_{ST} and K_{ST} are stripped values of U, Th and K.

Reduction to Standard Temperature and Pressure

The radar altimeter data were converted to effective height (H_{STP}) using the acquired temperature and pressure data, according to the expression:

$$H_{STP} = H \cdot \frac{273.15}{T + 273.15} \cdot \frac{P}{1013.25} \quad (14)$$

where H is the smoothed observed radar altitude in meters, T is the measured air temperature in degrees Celsius and P is the measured barometric pressure in millibars.

Height correction

Variations caused by changes in the aircraft altitude relative to the ground was corrected to a nominal height of 60 m. Data recorded at the height above 150 m were considered as non-reliable and removed from processing. Total count, Uranium, Thorium and Potassium stripped channels were subjected to height correction according to the equation:

$$C_{60m} = C_{ST} \cdot e^{C_{ht} \cdot (60 - H_{STP})} \quad (15)$$

where C_{ST} is the stripped corrected channel, C_{ht} is the height attenuation factor for that channel and H_{STP} is the effective height.

Conversion to ground concentrations

Finally, corrected count rates were converted to effective ground element concentrations using calibration values derived from calibration pads (Grasty et al. 1991) at the Geological Survey of Norway in Trondheim (see values in Appendix A2). The corrected data provide an estimate of the apparent surface concentrations of Potassium, Uranium and Thorium (K, eU and eTh). Potassium concentration is expressed as a percentage, equivalent Uranium and Thorium as parts per million (ppm). Uranium and Thorium are described as “equivalent” since their presence is inferred from gamma-ray radiation from daughter elements (^{214}Bi for Uranium, ^{208}Tl for Thorium). The concentration of the elements is calculated according to the following expressions:

$$C_{CONC} = C_{60m} / C_{SENS_60m} \quad (16)$$

where C_{60m} is the height corrected channel, C_{SENS_60m} is experimentally determined sensitivity reduced to the nominal height (60m).

Spectrometry data gridding and presentation

Gamma-rays from Potassium, Thorium and Uranium emanate from the uppermost 30 to 40 centimetres of soil and rock in the crust (Minty 1997). Variations in the concentrations of these radioelements largely related to changes in the mineralogy and geochemistry of the Earth’s surface.

The calculated ground concentrations of the three main natural radioelements Potassium, Thorium and Uranium and total gamma-ray flux (total count) were micro-levelled to remove small line-to-line levelling errors, as in the case of the magnetic data, and then gridded using a minimum curvature method with a grid cell size of 50 meters. This cell size is equal to one quarter of the 200m average line spacing.

A 3x3 convolution filter was applied to smooth the concentration grids. A list of the produced maps is shown on Table 5.

Quality of the radiometric data was within standard NGU specifications (Rønning 2013).

A list of the parameters used in the processing schemes is given in Appendix A2. For further reading regarding standard processing of airborne radiometric data, we recommend the publication from Minty et al. (1997).

4. PRODUCTS

Processed digital data from the survey are presented as:

1. Geosoft XYZ files:
 - Telemark_2015_Magnetics.XYZ
 - Telemark_2015_Radiometrics.XYZ
2. Georeferenced tiff files (Geo-tiff).
3. Coloured maps (jpg) at the scale 1:100.000 are available from NGU on request (see Table 5.).
- 4.

Table 5. Maps available from NGU on request.

Region	Map #	Scale	Name
Kviteseid, Nissedal, Fyresdal and Dalen	2015.040-01	1:100.000	Flight path
	2015.040-02	1:100.000	Total field magnetic anomaly
	2015.040-03	1:100.000	Magnetic Horizontal Derivative
	2015.040-04	1:100.000	Magnetic Vertical Derivative
	2015.040-05	1:100.000	Magnetic Tilt Derivative
	2015.040-06	1:100.000	Radiometry Total Counts
	2015.040-07	1:100.000	Potassium ground concentration
	2015.040-08	1:100.000	Uranium ground concentration
	2015.040-09	1:100.000	Thorium ground concentration
	2015.040-10	1:100.000	Radiometric Ternary Map

Downscaled images of the maps are shown on figures 4 to 13.

5. REFERENCES

Geosoft 2013: Getting Started with montaj GridKnit, Extension for Oasis Montaj v 8.0, Geosoft Corporation

Grasty, R.L., Holman, P.B. & Blanchard 1991: Transportable Calibration pads for ground and airborne Gamma-ray Spectrometers. Geological Survey of Canada, Paper 90-23: 62 pp.

IAEA 1991: Airborne Gamma-Ray Spectrometry Surveying, Technical Report No 323, Vienna, Austria, 97 pp.

IAEA 2003: Guidelines for radioelement mapping using gamma ray spectrometry data. IAEA-TECDOC-1363, Vienna, Austria, 173 pp.

Minty, B.R.S. 1997: The fundamentals of airborne gamma-ray spectrometry. AGSO Journal of Australian Geology and Geophysics, 17 (2): 39-50.

Minty, B.R.S., Luyendyk, A.P.J. and Brodie, R.C. 1997: Calibration and data processing for gamma-ray spectrometry. AGSO Journal of Australian Geology and Geophysics, 17(2): 51-62.

Naudy, H. and Dreyer, H. 1968: Non-linear filtering applied to aeromagnetic profiles. Geophysical Prospecting, 16(2): 171-178.

Rønning, J.S. 2013: NGUs helikoptermålinger. Plan for sikring og kontroll av datakvalitet. NGU Intern rapport 2013.001, (38 sider).

P1: Photo by Mari Nymoene, Telen Newspaper, Notodden

6. APPENDIX

A1: Flow chart of magnetic processing

Meaning of parameters is described in the referenced literature.

Processing flow:

- Quality control.
- Visual inspection of airborne data and manual spike removal
- Inspection of basemag data and removal of spikes
- Import basemag data to Geosoft database
- Correction of data for diurnal variation and IGRF
- Splitting flight data by lines
- Gridding
- Micro-leveling
- 5x5 convolution filter

A2: Flow chart of radiometry processing

Underlined processing stages are applied to the K, U, Th and TC windows.
Meaning of parameters is described in the referenced literature.

Processing flow:

- Quality control
- Airborne and cosmic correction (IAEA, 2003)
Used parameters: determined by high altitude calibration flights (1500-9000 ft) at Langøya in 2013

Channel	Background	Cosmic
K	7.3314	0.0617
U	0.8981	0.0454
Th	0.8881	0.0647
Uup	0.3926	0.0423
Total counts	36.291	1.0379

- Radon correction using upward detector method (IAEA, 2003)

Used parameters determined from survey data over water and land at Kviteseid, Nissedal, Fyresdal and Dalen in June 2015

Coefficient	Value	Coefficient	Value
a_u	0.2408	b_u	0.18235
a_K	0.83989	b_K	1.72692
a_{Th}	0.03852	b_{Th}	0.46439
a_{TC}	16.72806	b_{TC}	5.65049
a_1	0.08002413	a_2	0.01531852

- Stripping correction (IAEA, 2003)
Used parameters determined from measurements on calibrations pads at NGU on April 2015

Coefficient	Value
a	0.046955
b	0
c	0
α	0.306511
β	0.479806
γ	0.820563

- Height correction to a height of 60 m
Parameters determined by high altitude calibration flights (100 – 700 ft). The average values from tests performed at Rombaken (2011), Frosta (2014) and Beitostølen (2015) were used. Attenuation factors in 1/m:

Channel	Attenuation factor
K	-0.010014
U	-0.007403
Th	-0.007170
TC	-0.008237

- Converting counts at 60 m heights to element concentration on the ground
Used parameters determined from measurements on calibrations pads at NGU on April 2015

Channel	Sensitivity
K (%/count)	0.00750326482
U (ppm/count)	0.08792840784
Th (ppm/count)	0.1531553425

- Microlevelling using Geosoft menu and smoothening by a convolution filtering

Microlevelling parameters	Value
De-corrugation cutoff wavelength (m)	1000
Cell size for gridding (m)	50
Naudy (1968) Filter length (m)	600



Figure 4: Flight path map

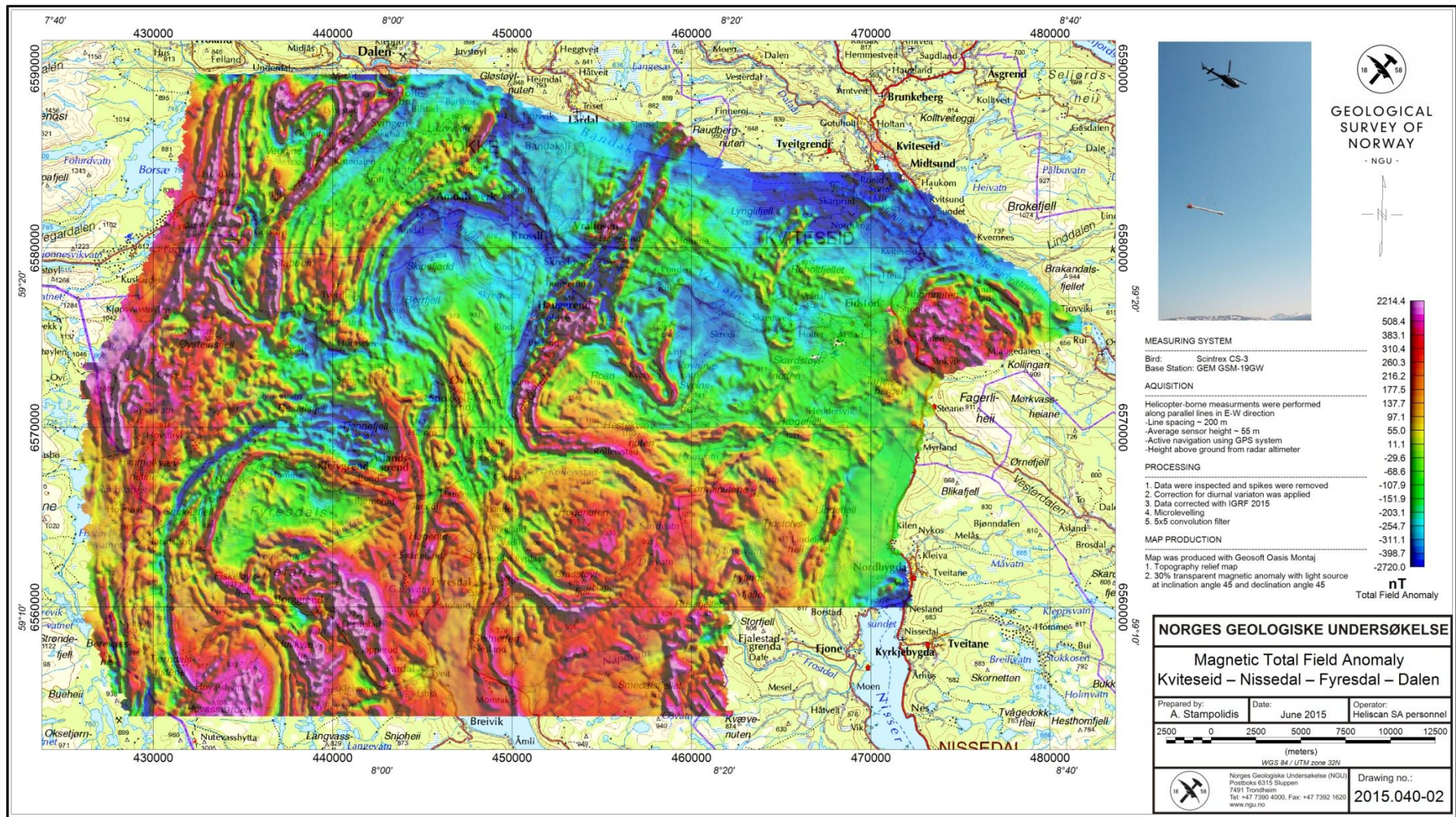


Figure 5: Total Magnetic Field anomaly map

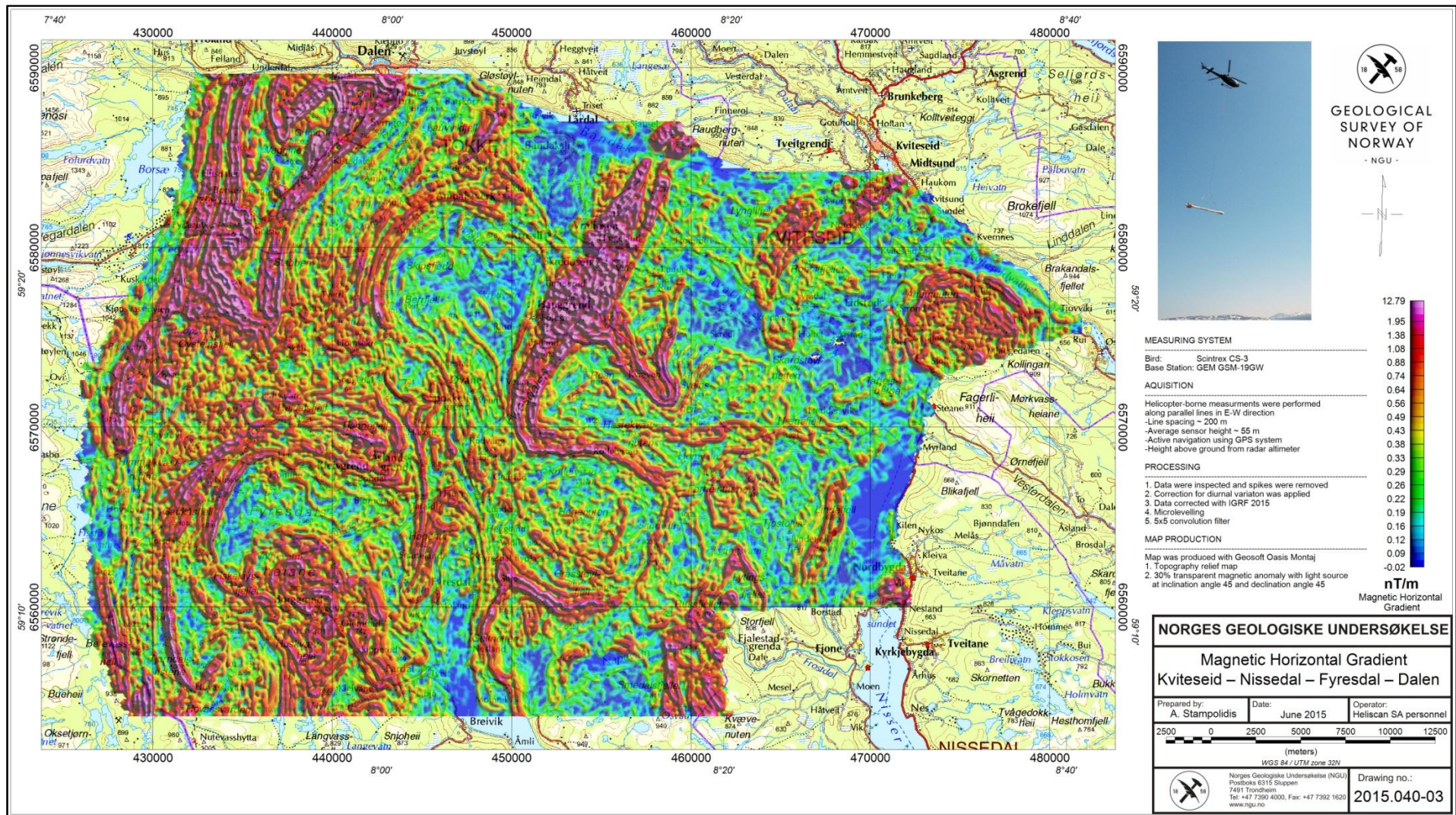


Figure 6: Magnetic Horizontal Gradient map

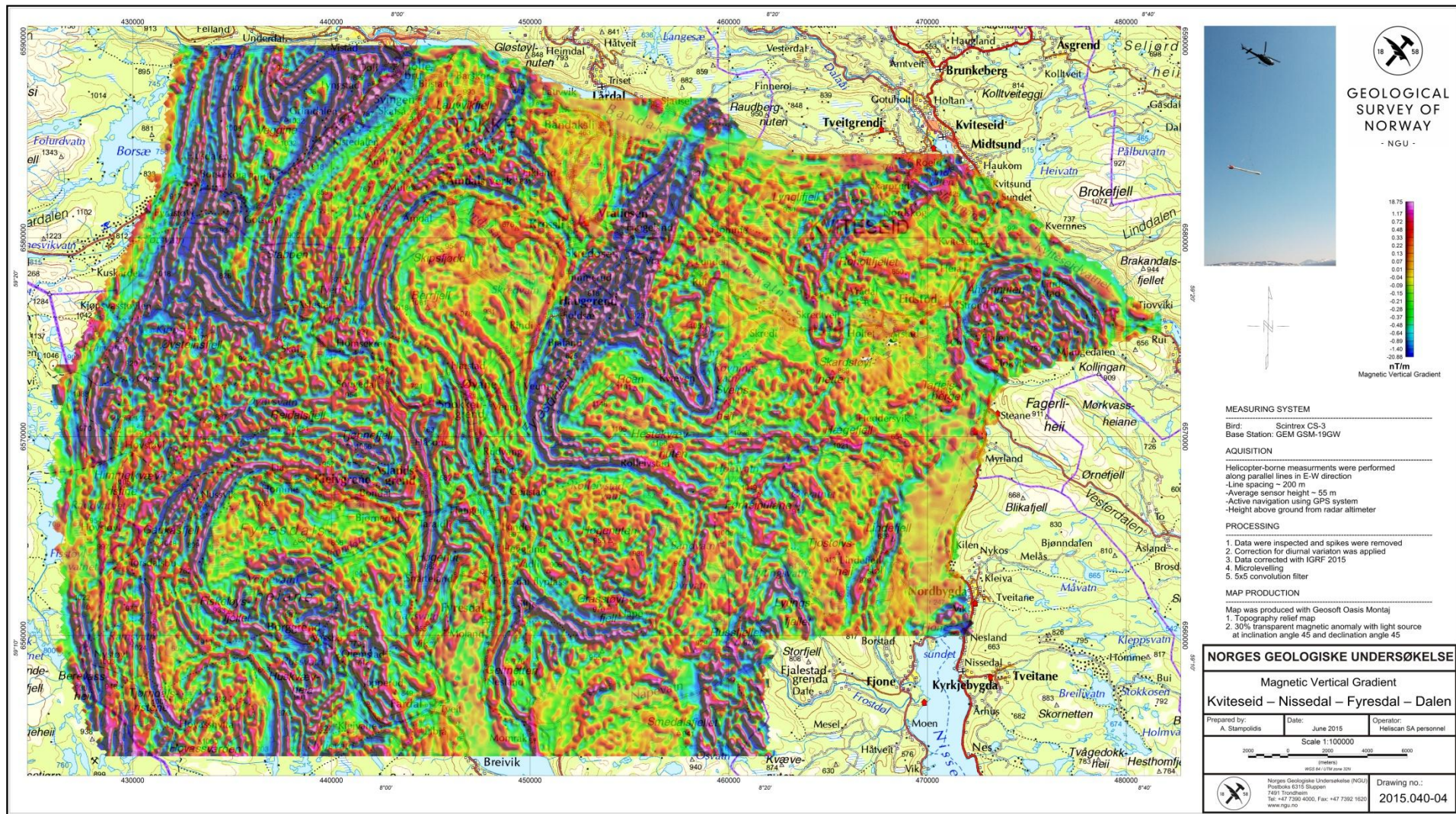


Figure 7: Magnetic Vertical Gradient map

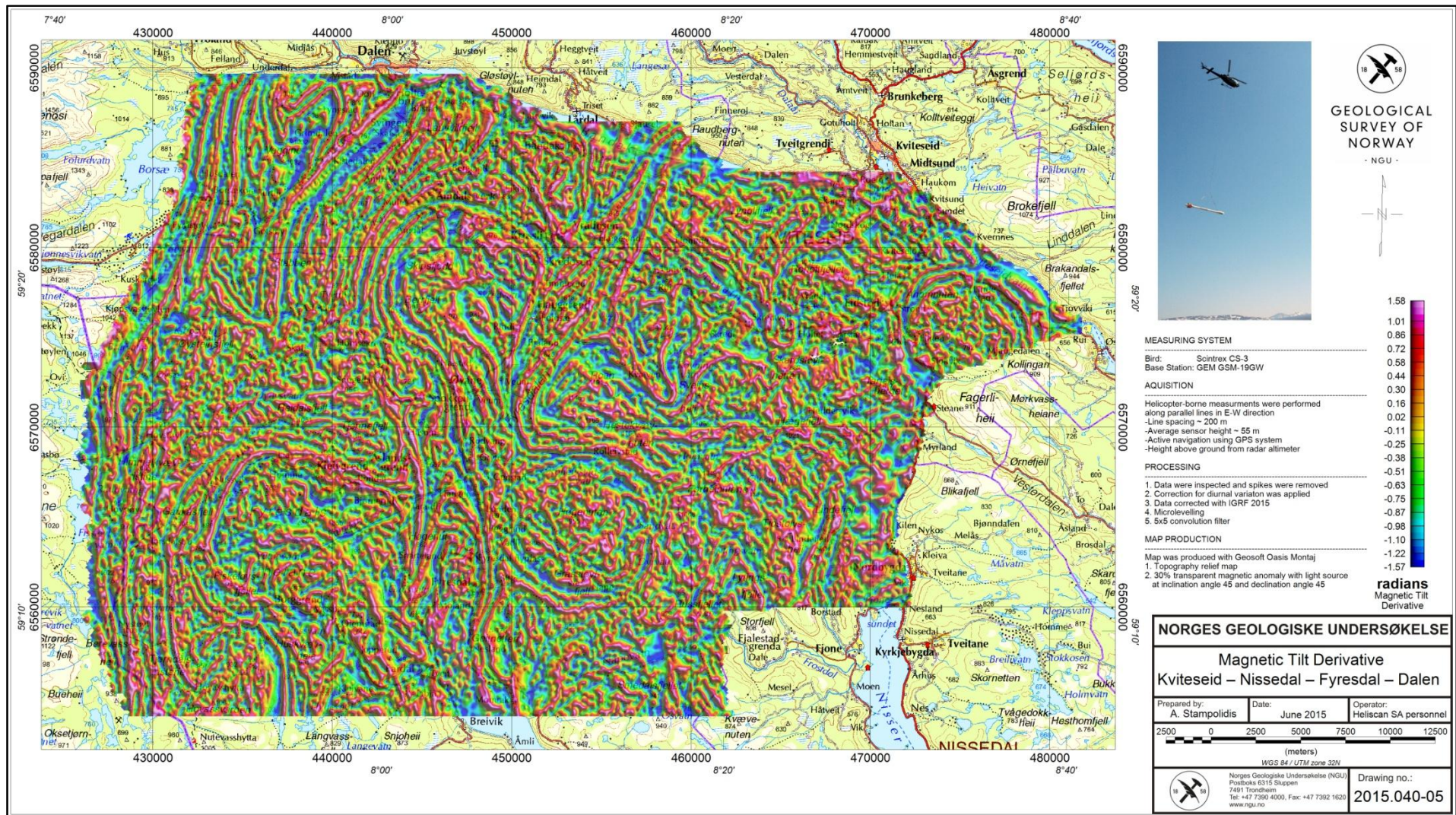


Figure 8: Magnetic Tilt Derivative map

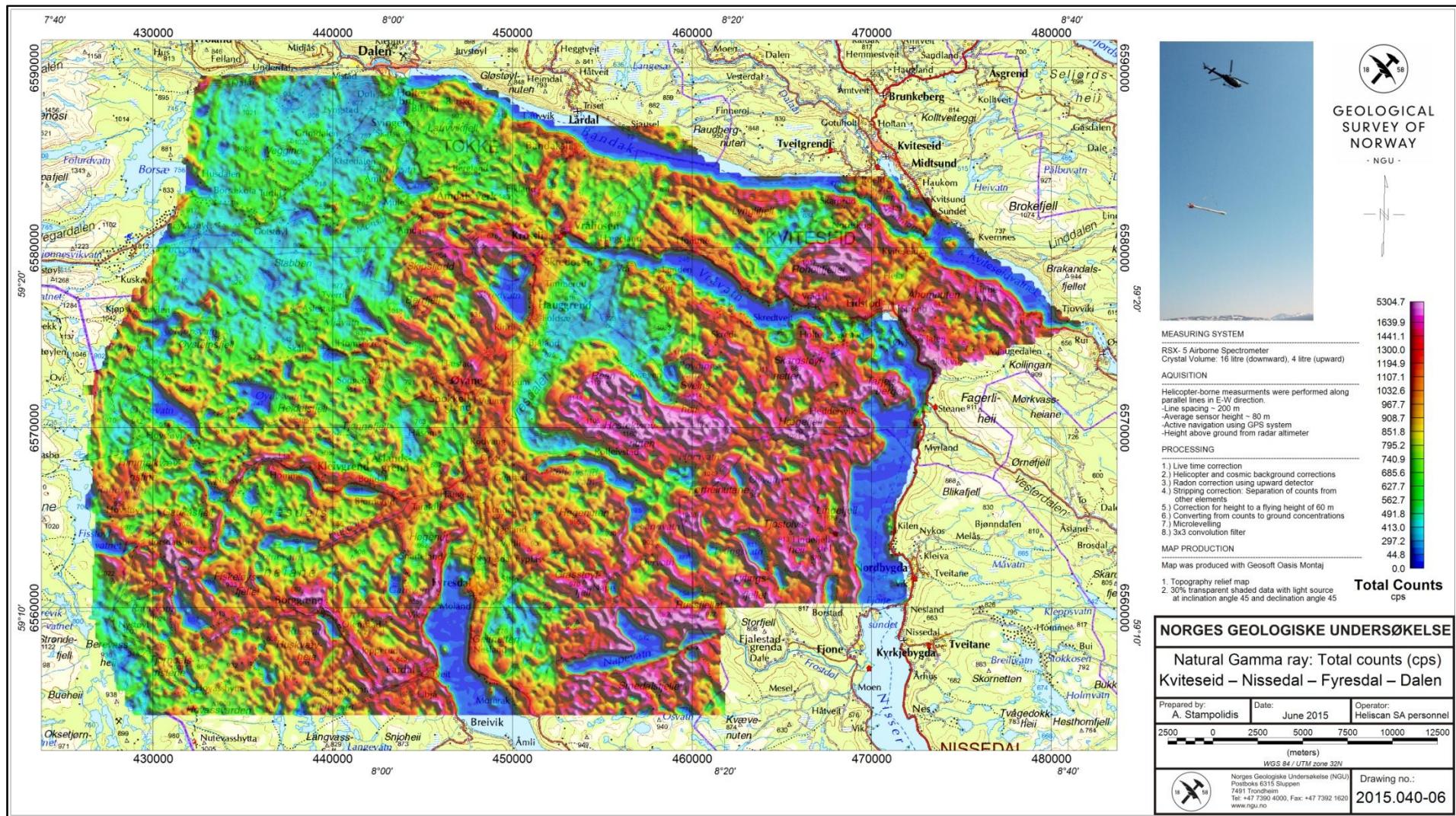


Figure 9: Radiometry: Total Counts map

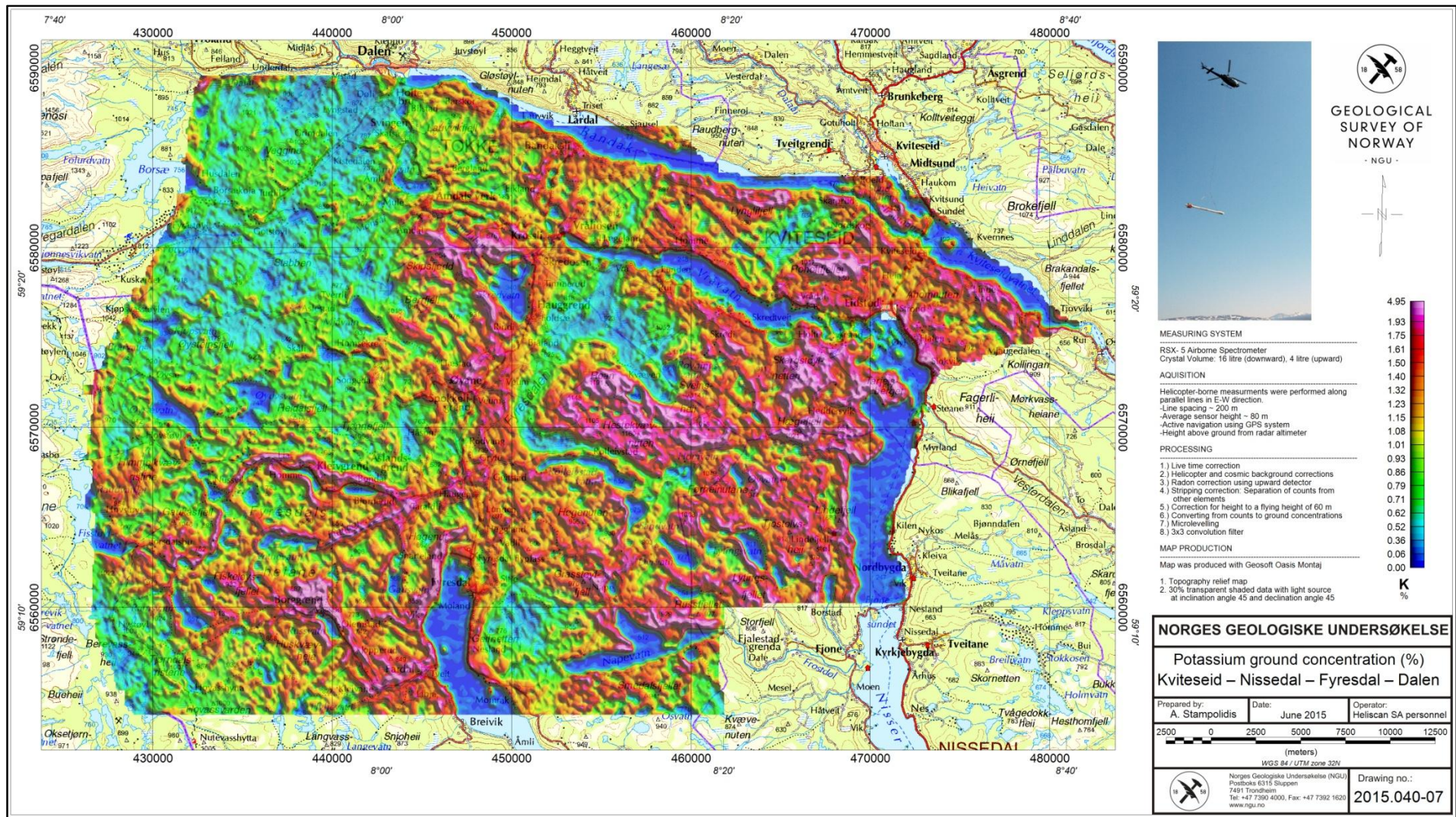


Figure 10: Potassium Ground Concentration map

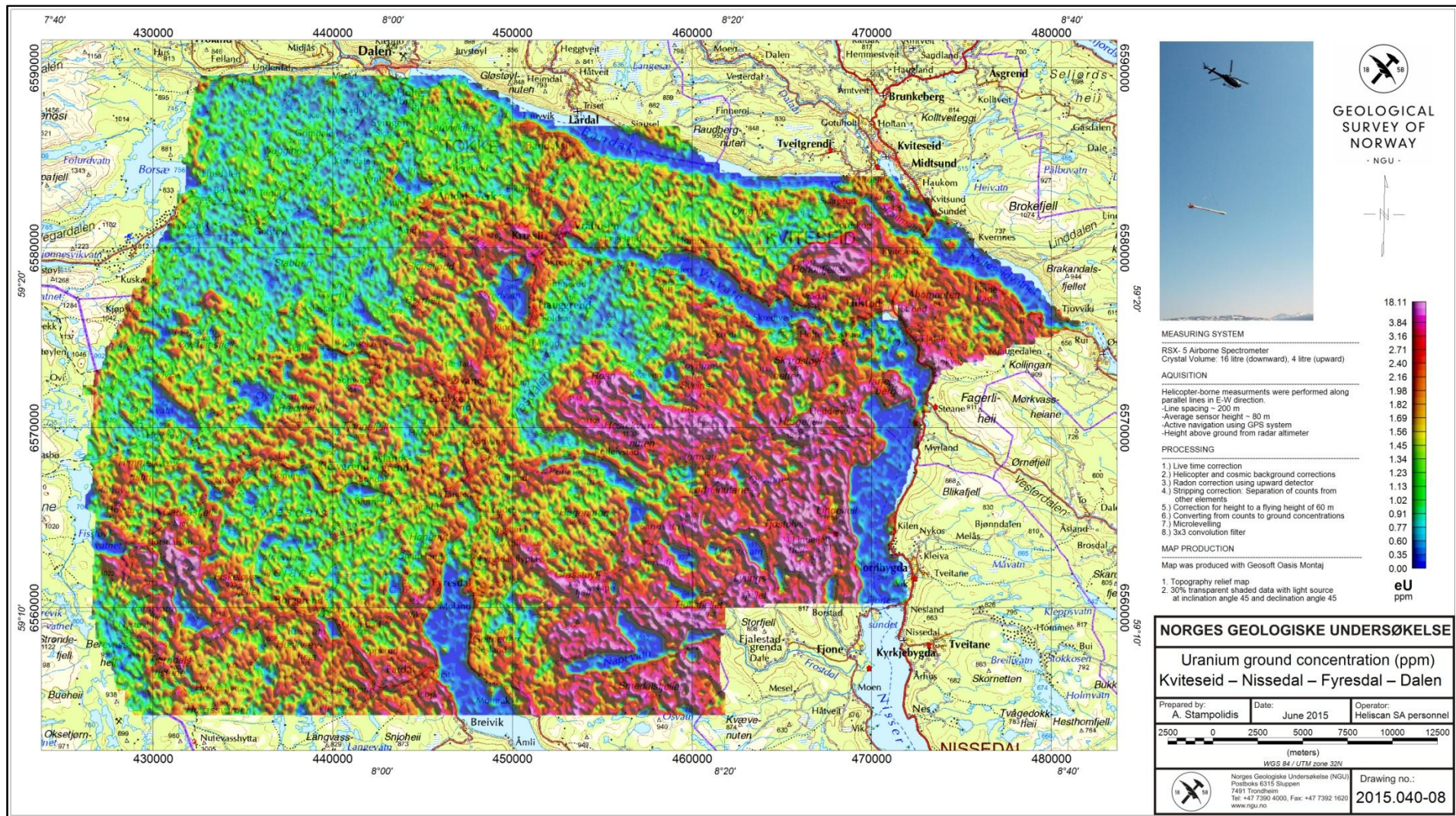


Figure 11: Uranium Ground Concentration map

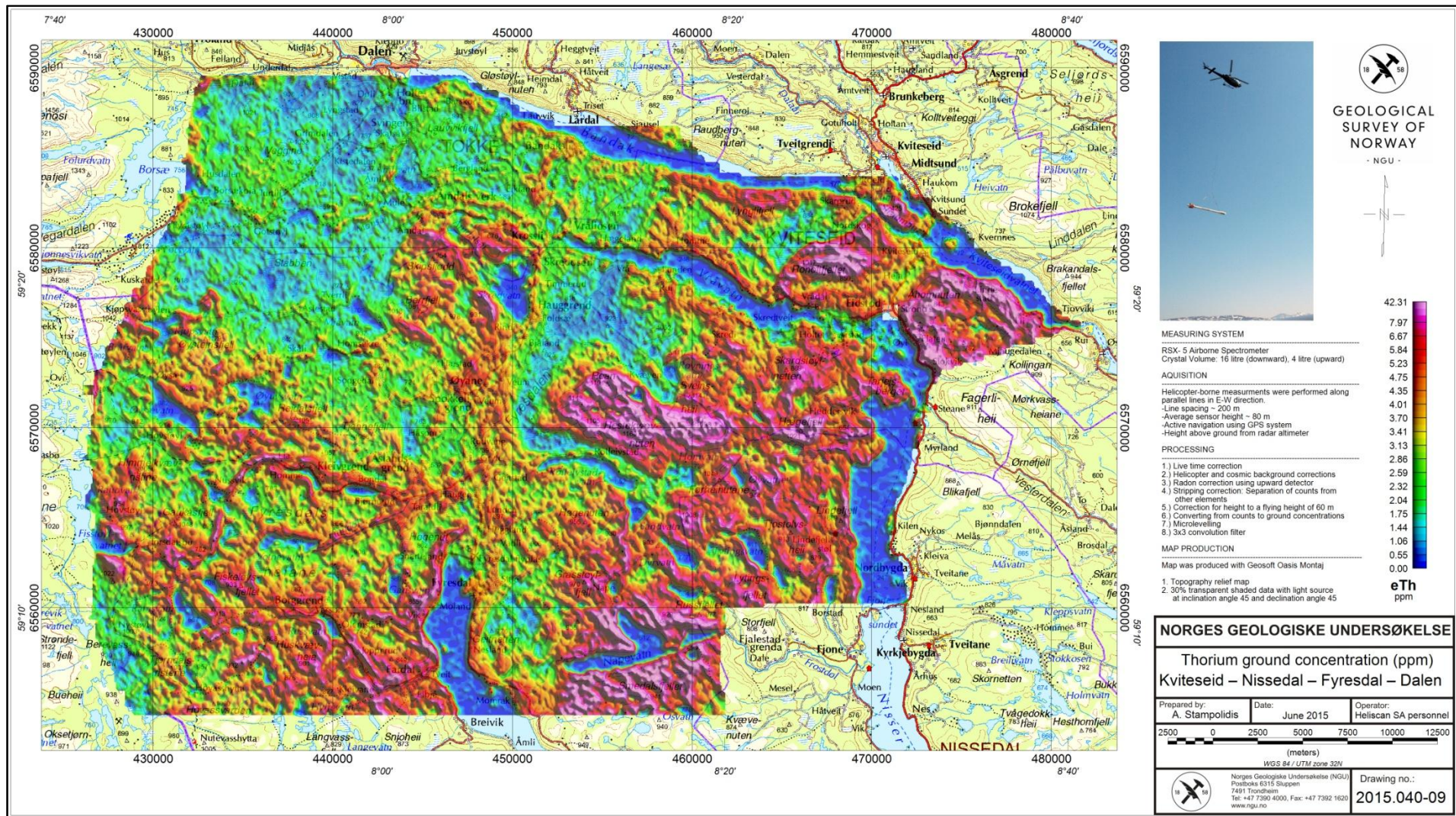


Figure 12: Thorium Ground Concentration map

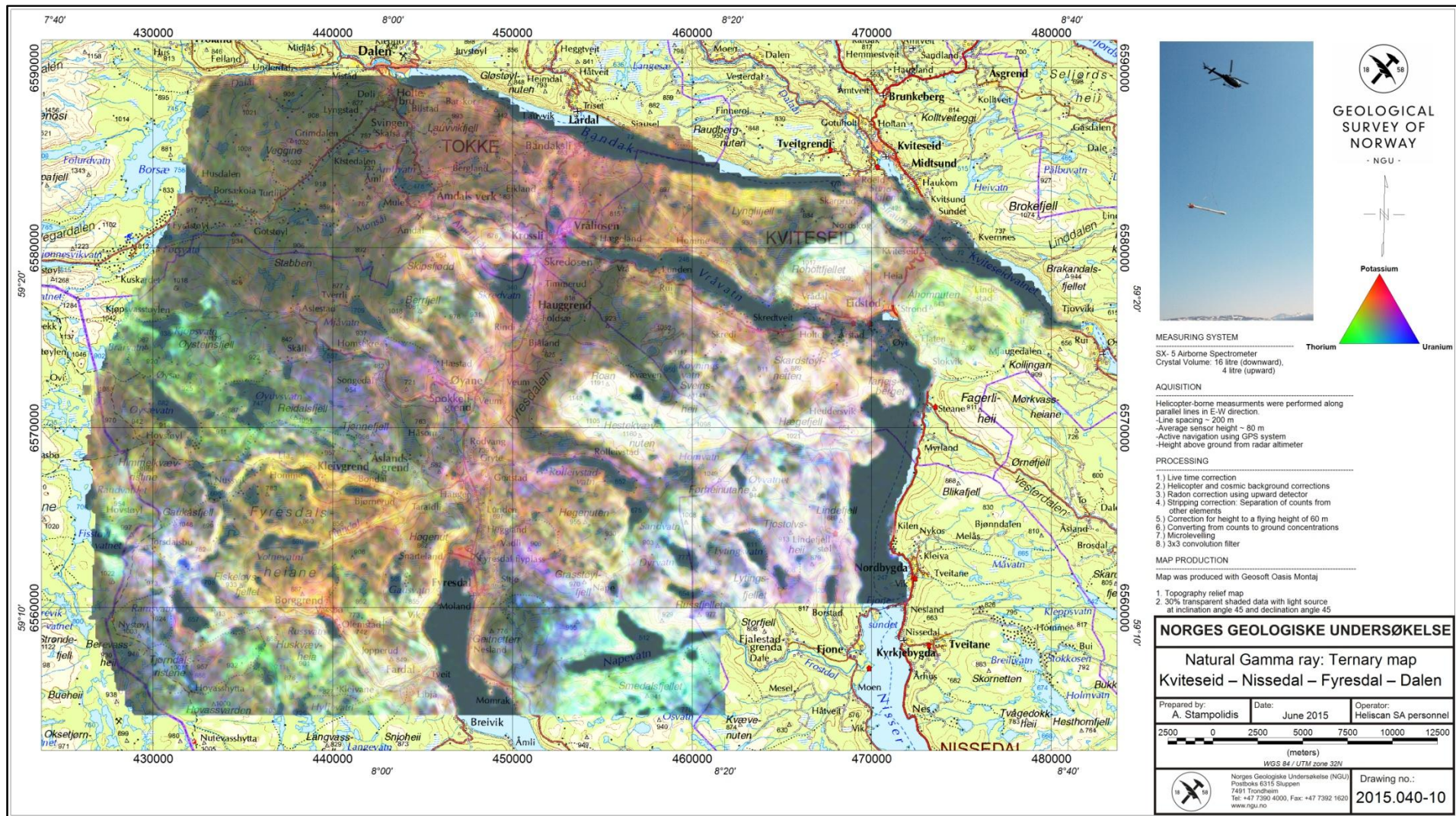


Figure 13: Ternary Image of Radiation Concentration